



Linear theory of electron temperature anisotropy instabilities: Whistler, mirror, and Weibel

S. Peter Gary¹ and Homa Karimabadi²

Received 4 April 2006; revised 12 June 2006; accepted 23 June 2006; published 21 November 2006.

[1] A collisionless, homogeneous plasma in which the electron velocity distribution is a bi-Maxwellian with $T_{\perp e} > T_{\parallel e}$, where the directional subscripts refer to directions relative to the background magnetic field \mathbf{B}_o , can support the growth of two distinct instabilities. Linear dispersion theory predicts that the whistler anisotropy instability is excited with maximum growth rate γ_m at $\mathbf{k} \times \mathbf{B}_o = 0$ and real frequency ω_r greater than the proton cyclotron frequency, whereas the electron mirror instability is excited at propagation oblique to \mathbf{B}_o and zero real frequency. In an unmagnetized plasma with a similarly anisotropic electron distribution the electron Weibel instability may be excited with zero real frequency and maximum growth rate in the direction of the minimum temperature. Here linear theory is used to compare dispersion and threshold properties of these three growing modes. For $0.10 \leq \beta_{\parallel e} \leq 1000$, the whistler has a larger γ_m and a smaller anisotropy threshold than the electron mirror, so that the former mode should dominate in homogeneous plasmas for most physical values of electron β . Threshold conditions describing electron temperature anisotropies and parallel wave numbers at given maximum growth rates are presented for each instability.

Citation: Gary, S. P., and H. Karimabadi (2006), Linear theory of electron temperature anisotropy instabilities: Whistler, mirror, and Weibel, *J. Geophys. Res.*, *111*, A11224, doi:10.1029/2006JA011764.

1. Introduction

[2] The collisionless tearing instability is often regarded as the primary onset mechanism for collisionless magnetic reconnection at the Earth's magnetopause and in the terrestrial magnetotail. Theory predicts that this instability is a sensitive function of the electron temperature anisotropy [e.g., Karimabadi *et al.*, 2004, and references therein], with $T_{\perp e}/T_{\parallel e} > 1$ yielding a substantial enhancement of this growth rate (The various symbols used here are defined in the Appendix.). Computer simulations of the tearing mode [Karimabadi *et al.*, 2004, 2005; Ricci *et al.*, 2004] have confirmed this prediction, suggesting that $T_{\perp e}/T_{\parallel e}$ is a critical parameter for determining the onset and saturation of collisionless reconnection.

[3] A possible source of electron anisotropy in a reconnection configuration has been demonstrated by Daughton *et al.* [2004]. Their particle-in-cell simulations of a current sheet in a collisionless plasma show that growth of the lower hybrid drift instability heats electrons in the directions perpendicular to the magnetic field. On the other hand, electron temperature anisotropies are limited in magnitude; theory and simulations of uniform magnetized plasmas have shown that the whistler anisotropy instability scatters electrons so as to impose a β_e -dependent upper bound on $T_{\perp e}/T_{\parallel e}$ [Gary and Wang, 1996; Gary *et al.*, 2000; Nishimura *et al.*,

2002] and recent observations demonstrate that this theoretical constraint is satisfied in the terrestrial magnetosheath [Gary *et al.*, 2005]. These considerations imply that to provide the proper context for application of electron temperature anisotropies to the tearing instability, it is appropriate to reexamine and compare the linear theory properties of the various short-wavelength resonant instabilities driven by this electron anisotropy.

[4] In a magnetized plasma there are two distinct electromagnetic instabilities driven by $T_{\perp e}/T_{\parallel e} > 1$ (Here e denotes electrons and the other subscripts indicate directions relative to the background magnetic field \mathbf{B}_o). The whistler anisotropy instability has been studied extensively through both linear theory [Kennel and Petschek, 1966; Scharer and Trivelpiece, 1967; Gary, 1993] and computer simulation [Ossakow *et al.*, 1972; Cuperman, 1981; Pritchett *et al.*, 1991; Devine *et al.*, 1995; Gary and Wang, 1996; Nishimura *et al.*, 2002]. The electron mirror instability has received less scrutiny [Pokhotelov *et al.*, 2002]; its name derives from the many properties it shares with the better known ion mirror instability driven by an ion $T_{\perp} > T_{\parallel}$. These common properties include $\omega_r = 0$ in a homogeneous plasma, maximum growth rate at propagation oblique to \mathbf{B}_o , predominantly compressive fluctuations, that is, $|\delta B_{\parallel}|^2 \gg |\delta B_{\perp}|^2$, and the Landau resonance of the anisotropic species as the primary wave-particle interaction of the instability.

[5] Electromagnetic growing modes driven by electron temperature anisotropies in an unmagnetized plasma are known as "Weibel instabilities" [Weibel, 1959]. For electron temperatures $T_x = T_y > T_z$, linear theory predicts [Kalman *et al.*, 1968; Yoon, 1989], and nonlinear theory [Montes *et al.*, 1970; Lemons and Winske, 1980] and computer simulations [Morse and Nielson, 1971; Lemons

¹Los Alamos National Laboratory, Los Alamos, New Mexico, USA.

²Department of Electrical and Computer Engineering, University of California, San Diego, La Jolla, California, USA.

Table 1. Electromagnetic Instabilities Driven by $T_{\perp e}/T_{\parallel e} > 1$

Instability	Magnetic Field	Real Frequency	Wave Vector at γ_m	
Whistler anisotropy	$\mathbf{B}_o \neq 0$	$\Omega_i < \omega_r < \Omega_e $	$k_m c/\omega_e < 1$	$\theta = 0^\circ$
Electron mirror	$\mathbf{B}_o \neq 0$	$\omega_r = 0$	$k_m c/\omega_e < 1$	$\theta \neq 0^\circ$
Electron Weibel	$\mathbf{B}_o = 0$	$\omega_r = 0$	$k_m c/\omega_e < 1$	$\theta = 0^\circ$

et al., 1979] are consistent with, an electron Weibel instability with $\omega_r = 0$ and maximum growth rate at propagation parallel to $\hat{\mathbf{z}}$. Table 1 summarizes selected properties of these three instabilities.

[6] Here linear theory in a homogeneous, collisionless plasma is used to compare dispersion and threshold properties of these growing modes. If the background magnetic field is nonzero, the general form of the dispersion equation at $\mathbf{k} \times \mathbf{B}_o = 0$ is

$$\omega^2 - k^2 c^2 + k^2 c^2 \sum_j S_j^\pm(\mathbf{k}, \omega) = 0$$

If the velocity distribution of each species j is represented as a single anisotropic bi-Maxwellian, it follows that [e.g., Gary, 1993]

$$S_j^\pm(\mathbf{k}, \omega) = \frac{\omega_j^2}{k^2 c^2} \left[\zeta_j Z(\zeta_j^\pm) + \left(1 - \frac{T_{\perp j}}{T_{\parallel j}}\right) \frac{Z'(\zeta_j^\pm)}{2} \right]$$

In the limit of $B_o = 0$, the dimensionless conductivity becomes

$$S_j(\mathbf{k}, \omega) = \frac{\omega_j^2}{k^2 c^2} \left[\zeta_j Z(\zeta_j) + \left(1 - \frac{T_{\perp j}}{T_{\parallel j}}\right) \frac{Z'(\zeta_j)}{2} \right]$$

[7] We consider two species: ions (denoted by subscript i) and electrons. We assume that the average relative drift between the electrons and ions is zero, and that charge neutrality $n_e = n_i$ holds. We assume the following dimensionless parameters: $m_i/m_e = 1836$, $T_{\parallel e}/T_{\parallel i} = 1$ and, to isolate the consequences of the electron anisotropy, $T_{\perp i}/T_{\parallel i} = 1$.

2. Dispersion

[8] Solutions of the linear dispersion equation for a collisionless plasma are typically expressed in terms of dimensionless variables. For the electron Weibel instability, it is natural to use the electron inertial length and the electron plasma frequency as normalizing factors; thus our results for this mode are described in terms of kc/ω_e and γ/ω_e . Then the dimensionless parameter which characterizes the electron temperature is $k_B T_{\parallel e}/m_e c^2$.

[9] For the whistler anisotropy and electron mirror instabilities, kc/ω_e is again an appropriate dimensionless variable, but frequencies and growth rates are usually normalized by the electron cyclotron frequency. In this case, the electron temperature is characterized by $\beta_{\parallel e}$, and dimensionless frequencies, growth rates, and wave numbers are essentially independent of $\omega_e/|\Omega_e|$ as long as this parameter is substantially greater than unity. For comparison of these

two magnetized instabilities, these normalizations are the natural ones to use.

[10] However, to compare all three instabilities, it is necessary to make the complex frequency dimensionless by dividing by ω_e . Then scaling relations for the magnetized instabilities should be constructed by varying both $\beta_{\parallel e}$ and $\omega_e/|\Omega_e|$ so that $k_B T_{\parallel e}/m_e c^2$ remains constant.

[11] Figure 1 compares growth rates for the three instabilities. Here and for a broad range of parameters the following ordering obtains

$$\begin{aligned} \gamma_m(\text{Electron mirror}) &< \gamma_m(\text{Whistler anisotropy}) \\ &\leq \gamma_m(\text{Electron Weibel}) \end{aligned}$$

Given that $\omega_r = 0$ for both the mirror and Weibel instabilities, one might expect that these two modes would display similar $\gamma(k)$. However, Figure 1 shows this is not the case; it is the $\gamma(k_{\parallel})$ of the whistler which closely resembles the Weibel growth rate.

[12] Figure 2 illustrates the growth rate maximized with respect to wave number and the corresponding wave number as a function of θ for the two modes in a magnetized plasma. This shows that $\gamma_m(\mathbf{k})$ lies at $\mathbf{k} \times \mathbf{B}_o = 0$ for the whistler and at $\theta \neq 0$ for the electron mirror instability.

3. Threshold Conditions

[13] This section describes several threshold conditions obtained from the linear theory of electron temperature

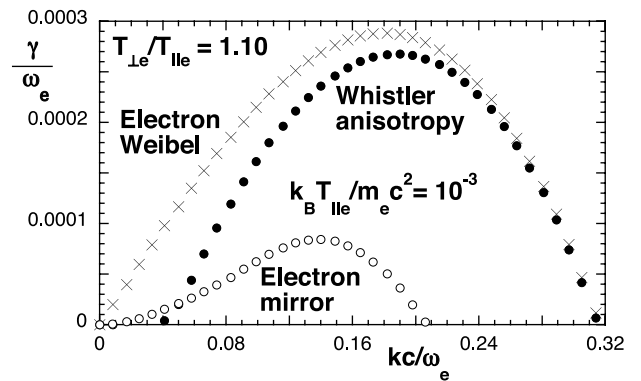


Figure 1. Growth rates of three electron temperature anisotropy instabilities at θ values corresponding to γ_m as functions of the fluctuation wave number. Results for the whistler anisotropy instability are at $\mathbf{k} \times \mathbf{B}_o = 0$ and are indicated by solid dots. Results for the electron mirror instability are at $\theta_m = 52^\circ$ and are indicated by open circles. Results for the electron Weibel instability are at $\mathbf{k} = \hat{\mathbf{z}}k$ and are shown as crosses. Here $k_B T_{\parallel e}/m_e c^2 = 10^{-3}$, and $T_{\perp e}/T_{\parallel e} = 1.10$. For the modes in a magnetized plasma, $\omega_e/|\Omega_e| = 223.57$, which implies $\beta_{\parallel e} = 100.0$.

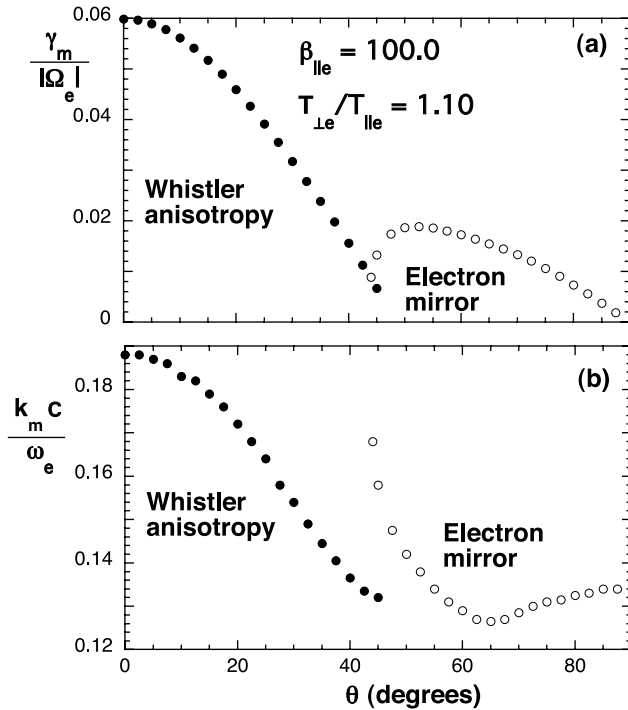


Figure 2. (a) Growth rates maximized over wave number at fixed θ and (b) corresponding wave numbers as functions of the direction of propagation for the whistler anisotropy and electron mirror instabilities. Here $\omega_e/|\Omega_e| = 223.57$, $\beta_{||e} = 100.0$, and $T_{\perp e}/T_{||e} = 1.10$.

anisotropy instabilities. We derive these threshold conditions in magnetized plasmas as follows. We first choose a value for the maximum dimensionless growth rate, e.g., $\gamma_m/|\Omega_e| = 0.01$. We next numerically solve the full linear dispersion equation for many values of $\beta_{||e}$, obtaining the corresponding frequencies, growth rates, and wave vectors for both the whistler anisotropy and the electron mirror instabilities. We find that the parallel wave number at maximum growth rate $k_{||m}c/\omega_e$ and the electron anisotropy $T_{\perp e}/T_{||e}$ are monotonically decreasing functions of $\beta_{||e}$ for both growing modes. Third, we carry out least squares fits of the wave number and the anisotropy as functions of $\beta_{||e}$ over limited ranges of the latter parameter.

[14] Gary and Wang [1996] showed that the linear theory threshold condition for the whistler anisotropy instability can be written as

$$\frac{T_{\perp e}}{T_{||e}} - 1 = \frac{S_e}{\beta_{||e}^{\alpha_e}} \quad (1)$$

where the fitting parameters S_e and α_e are functions of the choice of maximum growth rate and the range of $\beta_{||e}$ values over which the fit is carried out. Figure 3a shows that the anisotropy threshold condition for both instabilities can be well fit to equation (1) over $10 \leq \beta_{||e} \leq 1000$ at $\gamma_m/|\Omega_e| = 0.01$; Tables 2a and 2b state the associated fitting parameters for three different values of the maximum growth rate. Figure 3a also demonstrates that the electron mirror instability threshold anisotropy is substantially higher than that of the cyclotron resonant whistler anisotropy instability

for $0.10 \leq \beta_{||e} \leq 1000$. We conclude that the latter mode should be the dominant electron temperature anisotropy instability for virtually all physical values of electron β , and the absence of space plasma observations of the electron mirror mode is consistent with this conclusion.

[15] It is instructive to compare these results to the threshold conditions of two electromagnetic instabilities driven by the proton anisotropy $T_{\perp p}/T_{||p} > 1$. Such conditions for both the proton cyclotron anisotropy instability and the proton mirror instability also satisfy equation (1) with subscripts p substituted for subscripts e . A major difference between the two pairs of modes, however, is that the threshold curves of the two proton anisotropy instabilities cross at $\beta_{||p} \simeq 7$ [Gary *et al.*, 1994], so that the proton mirror mode has the faster growth rate and is likely to be the more important source of enhanced fluctuations at this and larger values of $\beta_{||p}$. This conclusion is supported by a number of space plasma observations of enhanced proton mirror fluctuations in the magnetosheath [e.g., Anderson *et al.*, 1994] as well as more indirect evidence for the excitation of the proton mirror mode in the solar wind [Winterhalter *et al.*, 1994].

[16] A second expression which emerges from linear dispersion theory describes the parallel wave number at instability threshold:

$$\frac{k_{||m}c}{\omega_e} = \frac{S_k}{\beta_{||e}^{\alpha_k}} \quad (2)$$

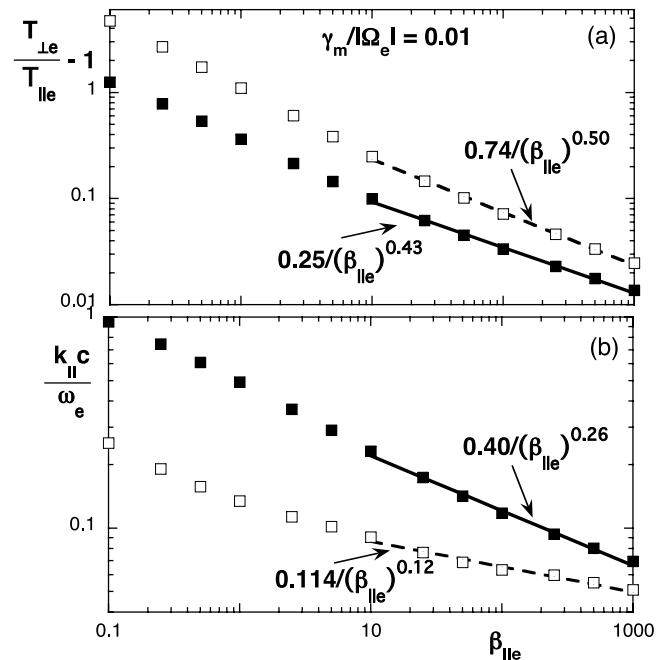


Figure 3. (a) Electron temperature anisotropy and (b) parallel dimensionless wave number at the $\gamma_m/|\Omega_e| = 0.01$ thresholds of two instabilities as functions of $\beta_{||e}$. In each case the discrete symbols represent linear theory results; the lines are least squares fits to these points over $10 \leq \beta_{||e} \leq 1000$. The solid symbols and the solid lines correspond to the whistler anisotropy instability; the open symbols and the dashed lines represent the electron mirror instability. Here $\omega_e/|\Omega_e| = 223.57$.

where the fitting parameters S_k and α_k are functions of the choice of maximum growth rate and the range of $\beta_{\parallel e}$ values over which the fit is carried out. Figure 3b shows that the wave number threshold condition for both instabilities can be well fit to equation (2) over $10 \leq \beta_{\parallel e} \leq 1000$ at $\gamma_m/|\Omega_e| = 0.01$; Tables 2a and 2b state the fitting parameters to equation (2) for three different values of the maximum growth rate.

[17] Figure 3b and Tables 2a and 2b imply that the parallel wave number of the electron mirror instability at a given threshold is universally smaller than the same quantity at threshold of the whistler anisotropy instability. Furthermore, Figure 1 suggests, and sample computations not described here confirm, that for a broad range of plasma parameters

$$k_{\parallel m}(\text{Electron mirror}) < k_m(\text{Electron Weibel}) \\ \leq k_{\parallel m}(\text{Whistler anisotropy})$$

[18] A third threshold condition is similar to the oft-quoted relationship for the electron Weibel instability $T_{\perp e}/T_{\parallel e} - 1 = (kc/\omega_e)^2$ [Lemons *et al.*, 1979; Yoon, 1989] which represents the maximum wave number available to growing fluctuations of this mode. (For example, see the short-wavelength cutoff illustrated in Figure 1.) Solutions of the linear dispersion equation yield a threshold condition for the electron Weibel instability:

$$\frac{T_{\perp e}}{T_{\parallel e}} - 1 = 3 \left(\frac{k_m c}{\omega_e} \right)^2 \quad (3)$$

for $k_m c/\omega_e \ll 1$. Further, we find this result to be independent of the value of $k_B T_{\parallel e}/m_e c^2$. Figure 4 illustrates this result and, furthermore, shows that it is approximately true for an intermediate range of wave numbers for the whistler anisotropy instability. At the relatively long wavelengths corresponding to weak anisotropies, ion cyclotron damping quenches the whistler anisotropy instability and equation (3) is no longer appropriate for that growing mode.

4. Conclusions

[19] We used linear theory for homogeneous, collisionless plasmas bearing a bi-Maxwellian electron velocity distribution with $T_{\perp e}/T_{\parallel e} > 1$ to compare the properties of three growing modes: the whistler anisotropy instability and the electron mirror instability in a magnetized plasma and the electron Weibel instability in an unmagnetized plasma. Over $0.10 \leq \beta_{\parallel e} \leq 1000$ the first two of these modes have anisotropy thresholds with the form of equation (1), although the whistler instability has the uniformly lower threshold.

Table 2a. Fitting Parameters to Threshold Conditions: Whistler Anisotropy Instability ($10 \leq \beta_{\parallel e} \leq 1000$)

$\gamma_m/ \Omega_e $	S_k	α_k	S_e	α_e
0.001	0.36	0.33	0.15	0.56
0.01	0.40	0.26	0.25	0.43
0.10	0.56	0.20	0.80	0.37

Table 2b. Fitting Parameters to Threshold Conditions: Electron Mirror Instability ($10 \leq \beta_{\parallel e} \leq 1000$)

$\gamma_m/ \Omega_e $	S_k	α_k	S_e	α_e
0.001	0.048	0.13	0.53	0.64
0.01	0.114	0.12	0.74	0.50
0.10	0.27	0.11	2.21	0.46

Similarly, the electron Weibel and whistler anisotropy instabilities satisfy the threshold condition equation (3).

[20] The threshold conditions described here may be useful proxies for describing the consequences of scattering by these relatively short wavelength modes. For example, if a plasma is magnetized with relatively weak gradients parallel to \mathbf{B}_0 , as may be the case in a plasma sheet with a so-called guide magnetic field, then the whistler will be the most important growing mode driven by this electron anisotropy. Particle-in-cell simulations have shown that this instability growth leads to electron scattering; a consequence of this scattering is to reduce the electron temperature anisotropy to or below the instability threshold condition. Then equation (1) with fitting parameters corresponding to an appropriate instability growth rate determines the maximum anisotropy which can be sustained under such conditions. Under the plausible assumption that instability growth and scattering rates are much faster than the growth rate of a large-scale instability such as the tearing mode, equation (1) then provides an upper bound on the $T_{\perp e}/T_{\parallel e}$ which, in turn, provides a limit on the tearing growth rate.

[21] The conclusions of this paper have been derived from a linear theory which assumes that the electrons may be represented in terms of a single bi-Maxwellian velocity distribution. Linear stability theory for more general electron distributions has been used to study both the whistler [e.g., *Cuperman*, 1981] and the mirror [Gedalin *et al.*, 2001; Pokhotelov *et al.*, 2002] instabilities. It would be useful to extend our detailed comparison of the various electron anisotropy instabilities to include non-Maxwellian effects, especially those which

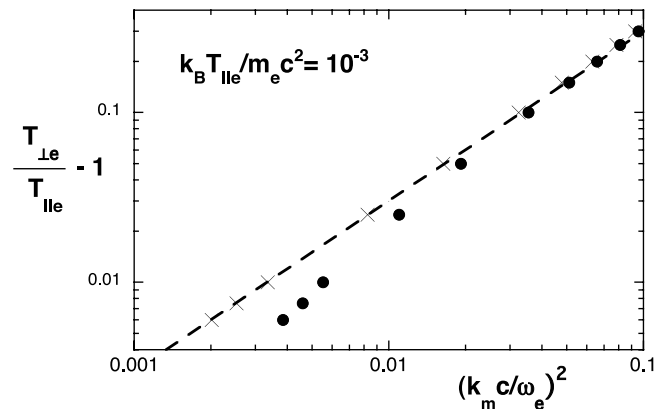


Figure 4. Electron temperature anisotropy at maximum growth rate as a function of the square of the wave number at maximum growth rate. The solid dots represent results for the whistler anisotropy instability, whereas the crosses represent results for the electron Weibel instability. The dashed line represents equation (3). Here $k_B T_{\parallel e}/m_e c^2 = 10^{-3}$. For the whistler, $\omega_e/|\Omega_e| = 223.57$, which implies $\beta_{\parallel e} = 100.0$.

may be associated with reconnection. However, spacecraft measurements of electron distributions and magnetic fields within diffusion regions are extremely difficult. Simulations indicate a nongyrotropic electron distribution in the antiparallel geometry and a gyrotropic distribution in the presence of a guide field. In the latter case the bi-Maxwellian assumption is accurate and in the former case it has been shown [Karimabadi *et al.*, 2005] that surprisingly, linear theory does a fairly good job of predicting linear growth even when the electrons are significantly nongyrotropic. Clearly, the issue of competition between various instabilities in the highly inhomogeneous setting of a current sheet requires further study and is beyond the scope of this work.

Appendix A: Definitions

[22] For the j th species we define $\beta_{\parallel j} \equiv 8\pi n_j k_B T_{\parallel j} / B_o^2$; the plasma frequency, $\omega_j \equiv \sqrt{4\pi n_j e_j^2 / m_j}$; the cyclotron frequency, $\Omega_j \equiv e_j B_o / m_j c$; and the thermal speed, $v_j \equiv \sqrt{k_B T_{\parallel j} / m_j}$. The complex frequency is $\omega = \omega_r + i\gamma$, the Landau resonance factor of the j th species is $\zeta_j \equiv \omega / \sqrt{2} |k_{\parallel}| v_j$, and the cyclotron resonance factors of the j th species are $\zeta_j^{\pm} \equiv (\omega \pm \Omega_j) / \sqrt{2} |k_{\parallel}| v_j$. The choice of coordinate system is such that both \mathbf{B}_o and the wave vector \mathbf{k} lie in the y - z plane. We define θ as the angle between \mathbf{k} and \mathbf{B}_o , so that $\hat{\mathbf{k}} \cdot \hat{\mathbf{B}}_o = \cos(\theta)$. Subscript m denotes a quantity corresponding to the maximum growth rate γ_m / Ω_i ; thus k_m and θ_m correspond to the wave vector which yields the largest value of γ for a given set of dimensionless plasma parameters.

[23] **Acknowledgments.** The work performed at Los Alamos National Laboratory was done under the auspices of the U.S. Department of Energy (DOE) and was supported by the DOE Office of Basic Energy Sciences, Division of Engineering and Geosciences, and the Sun-Earth Connection Theory Program of the National Aeronautics and Space Administration. H. Karimabadi's research was supported by NASA Geospace Sciences SR&T award NNG05GJ25G.

[24] Amitava Bhattacharjee thanks Mikhail Medvedev and Richard Sydora for their assistance in evaluating this paper.

References

- Anderson, B. J., S. A. Fuselier, S. P. Gary, and R. E. Denton (1994), Magnetic spectral signatures in the Earth's magnetosheath and plasma depletion layer, *J. Geophys. Res.*, *99*, 5877.
- Cuperman, S. (1981), Electromagnetic kinetic instabilities in multicomponent space plasmas: Theoretical predictions and computer simulation experiments, *Rev. Geophys.*, *19*, 307.
- Daughton, W., G. Lapenta, and P. Ricci (2004), Nonlinear evolution of the lower-hybrid drift instability in a current sheet, *Phys. Rev. Lett.*, *93*, 105004.
- Devine, P. E., S. C. Chapman, and J. W. Eastwood (1995), One- and two-dimensional simulations of whistler mode waves in an anisotropic plasma, *J. Geophys. Res.*, *100*, 17,189.
- Gary, S. P. (1993), *Theory of Space Plasma Microinstabilities*, Cambridge Univ. Press, New York.
- Gary, S. P., and J. Wang (1996), Whistler instability: Electron anisotropy upper bound, *J. Geophys. Res.*, *101*, 10,749.
- Gary, S. P., B. J. Anderson, R. E. Denton, S. A. Fuselier, and M. E. McKean (1994), A limited closure relation for anisotropic plasmas from the Earth's magnetosheath, *Phys. Plasmas*, *1*, 1676.
- Gary, S. P., D. Winske, and M. Hesse (2000), Electron temperature anisotropy instabilities: Computer simulations, *J. Geophys. Res.*, *105*, 10,751.
- Gary, S. P., B. Lavraud, M. F. Thomsen, B. Lefebvre, and S. J. Schwartz (2005), Electron anisotropy constraint in the magnetosheath: Cluster observations, *Geophys. Res. Lett.*, *32*, L13109, doi:10.1029/2005GL023234.
- Gedalin, M., Y. E. Lyubarsky, M. Balikhin, and C. T. Russell (2001), Mirror modes: Non-Maxwellian distributions, *Phys. Plasmas*, *8*, 2934.
- Kalman, G., C. Montes, and D. Quemada (1968), Anisotropic temperature plasma instabilities, *Phys. Fluids*, *11*, 1797.
- Karimabadi, H., W. Daughton, and K. B. Quest (2004), Role of electron temperature anisotropy in the onset of magnetic reconnection, *Geophys. Res. Lett.*, *31*, L18801, doi:10.1029/2004GL020791.
- Karimabadi, H., W. Daughton, and K. B. Quest (2005), Physics of saturation of collisionless tearing mode as a function of guide field, *J. Geophys. Res.*, *110*, A03214, doi:10.1029/2004JA010749.
- Kennel, C. F., and H. E. Petschek (1966), Limit on stably trapped particle fluxes, *J. Geophys. Res.*, *71*, 1.
- Lemons, D. S., and D. Winske (1980), Statistical thermodynamics of temperature anisotropy driven Weibel instabilities, *J. Plasma Phys.*, *23*, 283.
- Lemons, D. S., D. Winske, and S. P. Gary (1979), Nonlinear theory of the Weibel instability, *J. Plasma Phys.*, *21*, 287.
- Montes, C., J. Coste, and G. Diener (1970), Relaxation of a temperature anisotropy in a collisionless plasma, *J. Plasma Phys.*, *4*, 21.
- Morse, R. L., and C. W. Nielson (1971), Numerical simulation of the Weibel instability in one and two dimensions, *Phys. Fluids*, *14*, 830.
- Nishimura, K., S. P. Gary, and H. Li (2002), Whistler anisotropy instability: Wave-particle scattering rate, *J. Geophys. Res.*, *107*(A11), 1375, doi:10.1029/2002JA009250.
- Ossakow, S. L., I. Haber, and E. Ott (1972), Simulation of whistler instabilities in anisotropic plasmas, *Phys. Fluids*, *15*, 1538.
- Pokhotelov, O. A., R. A. Treumann, R. Z. Sagdeev, M. A. Balikhin, O. G. Onishchenko, V. P. Pavlenko, and I. Sandberg (2002), Linear theory of the mirror instability in non-Maxwellian space plasmas, *J. Geophys. Res.*, *107*(A10), 1312, doi:10.1029/2001JA009125.
- Pritchett, P. L., D. Schriver, and M. Ashour-Abdalla (1991), Simulation of whistler waves excited in the presence of a cold plasma cloud: Implications for the CRRES mission, *J. Geophys. Res.*, *96*, 19,507.
- Ricci, P., J. U. Brackbill, W. Daughton, and G. Lapenta (2004), New role of the lower hybrid drift instability in the magnetic reconnection, *Phys. Plasmas*, *12*, 055901.
- Scharer, J. E., and A. W. Trivelpiece (1967), Cyclotron wave instabilities in a plasma, *Phys. Fluids*, *10*, 591.
- Weibel, E. S. (1959), Spontaneously growing transverse waves in a plasma due to an anisotropic velocity distribution, *Phys. Rev. Lett.*, *2*, 83.
- Winterhalter, D., M. Neugebauer, B. E. Goldstein, E. J. Smith, S. J. Bame, and A. Balogh (1994), Ulysses field and plasma observations of magnetic holes in the solar wind and their relation to mirror-mode structures, *J. Geophys. Res.*, *99*, 23,371.
- Yoon, P. H., (1989) Electromagnetic Weibel instability in a fully relativistic bi-Maxwellian plasma, *Phys. Fluids B*, *1*, 1336.
- S. P. Gary, Los Alamos National Laboratory, Mail Stop D466, Group ISR-1, Los Alamos, NM 87545, USA. (pgary@lanl.gov)
- H. Karimabadi, Department of Electrical and Computer Engineering, University of California, San Diego, La Jolla, CA 92093-0407, USA. (homa@ece.ucsd.edu)